Structure factors of polydisperse systems of hard spheres: A comparison of Monte Carlo simulations and Percus–Yevick theory

D. Frenkel
Physical Laboratory, University of Utrecht, Princetonplein 5, Utrecht, the Netherlands
R. J. Vos, C. G. de Kruif, and A. Vrij
Van't Hoff Laboratory, University of Utrecht, Padualaan 8, Utrecht, the Netherlands

(Received 28 October 1985; accepted 18 December 1985)

We present Monte Carlo (MC) simulations of the structure factors of polydisperse hard-sphere fluids. The simulations were carried out for 108 particles and packing fractions up to $\phi = 0.5$. The size distribution of the particles was chosen randomly from a log-normal distribution. The MC results are compared with predictions obtained using Percus–Yevick approximation. It is found that for all but the highest densities and the highest polydispersities studied, the Percus–Yevick approximation provides a satisfactory description of the MC data.

I. INTRODUCTION

Scattering of electromagnetic radiation and (cold) neutrons is becoming a tool of increasing importance in the study of "supramolecular liquid structures" in concentrated solutions of colloidal particles dispersed in a low-molecular liquid.[1] In analyzing the data one usually assumes that the interacting particles are uniform in size and shape and that the interaction forces between the particles are identical. This is of course an oversimplification. Colloidal particles are prepared in such a way that because of the nature of their preparation, there will always be a distribution in these parameters. In practice one can synthesize colloidal spheroids with mean diameters of between 50 and 500 nm and a standard deviation ranging from 5% for the largest spheroids to 20% for the smallest ones.[2] Particles that are formed spontaneously in a solution (e.g., a microemulsion of water droplets dispersed in an oil and stabilized with surfactants) also vary in size, sometimes by as much as 30%.[3]

In dilute colloidal suspensions, where the interactions between particles are negligible, scattering methods have been used for a long time to analyze the particle configurations. In nondilute systems, where the interaction forces between particles cannot be neglected, the situation is much more complicated and therefore much more difficult to analyze. It is often assumed that in such systems the interactions between particles are identical although the scattering properties of the particles may still vary.[4,5] But pair potentials of different particle pairs usually will not all be the same and will show smaller or larger variations in magnitude and range. It is therefore very desirable to consider a model system where the effects of polydispersity in interaction parameters can be described by an approximate analytical theory.

A simple model potential for which this is feasible is the "hard-sphere" pair potential. This potential is also quite realistic in certain colloid systems.[6] The potential is characterized by only a single parameter: the hard-sphere diameter d. The attractive feature of this system is that an approximate theory is available to describe its structural and thermodynamic properties. This theory is based on using the Percus–Yevick approximation in the Ornstein–Zernike equation and was developed by Lebowitz[7] and Baxter.[8] In principle it allows one to evaluate the radial distribution functions of the different particle pairs in a hard-sphere mixture. From the results one may also calculate the intensity scattered by a mixture of particles with hard-sphere interactions as a function of scattering angle. Fortunately, this can even be done in a closed form so that after the Percus–Yevick approximation has been adopted the scattering can be evaluated exactly[9,10] for all types of polydispersities in particle scattering properties and interaction (hard-sphere sizes). Explicit results were obtained by Van Beurten and Vrij.[11] They used a Schulz distribution of hard-sphere sizes with standard deviations of up to 100% and different particle scattering functions.

From earlier computer simulations on fluids of monodisperse hard spheres it is known that the Percus–Yevick approximation yields a reasonable description of the static structure factor up to the freezing density.[12] It is not known, how accurately the Percus–Yevick approximation describes the scattering properties of polydisperse fluids.

In this paper we give some first results of Monte Carlo simulations and compare these with calculations based on the multicomponent Percus–Yevick solution.

II. SCATTERING EQUATIONS

A. Scattering amplitudes of particles

We consider a p-component system of particles dispersed in a solvent. The scattering amplitude contributed by a particle i will be denoted by $f_i B_i(K)$. Here f_i is the amplitude at zero angle of scattering and $B_i(K)$ is their normalized intraparticle interference factor and is unity at $K = 0$. $B_i(K)$ and f_i are given by[9]:

$$B_i(K) = f_i^{-1} 4\pi \int_0^\infty r^2 \zeta_i(r) \frac{\sin Kr}{Kr} dr , \tag{1}$$

$$f_i = 4\pi \int_0^\infty r^2 \zeta_i(r) dr . \tag{2}$$

Here $\zeta_i(r)$ is the (spherosymmetric) distribution of scattering material inside particle i, and K is the magnitude of the scattering vector given by $K = (4\pi/\lambda)\sin(\theta/2)$ with λ the wavelength of the scattering radiation and θ the scattering angle.

 0021-9606/86/084625-06$02.10

Nonspherosymmetric distributions can also be treated but they do not add any essentially new feature and fall outside the scope of this paper.

B. Scattering Intensity

The scattering intensity per unit volume of the particle dispersion is given by[9,13]:

$$R(K) = \sum_{i,k=1}^{p} f_i f_k B_i(K) B_k(K) (\rho_i \rho_k)^{1/2} [\delta_{ik} + \tilde{H}_{ik}(K)] \tag{3}$$

with

$$\tilde{H}_{ik}(K) = (\rho_i \rho_k)^{1/2} \int_0^\infty 4\pi r^2 h_{ik}(r) \left[\frac{\sin(Kr)}{Kr}\right] dr . \tag{4}$$

Here $h_{ik}(r) = g_{ik}(r) - 1$, where $g_{ik}(r)$ is the radial distribution function of the pair i, k, and r is the distance between the particle (force) centers. Further ρ_i and ρ_k are the number densities of the particle species i and k, and δ_{ik} is the Kronecker delta ($\delta_{ik} = 0$ when $i \neq k$ and $\delta_{ik} = 1$ when $i = k$). The functions $\tilde{H}_{ik}(K)$ describe the interparticle interference effects on the scattering. For low enough particle concentrations ($\rho_i \to 0$) the $\tilde{H}_{ik}(K)$ vanish and Eq. (3) becomes simply

$$R_0(K) = \sum_{i=1}^{p} \rho_i f_i^2 B_i^2(K) . \tag{5}$$

For a single component fluid (i.e., $p = 1$) Eq. (3) reduces to

$$R(K) = \rho f^2 P(K) S(K) \tag{6}$$

with

$$P(K) = B^2(K) \tag{7}$$

and

$$S(K) = 1 + \tilde{H}(K) = 1 + \rho \int_0^\infty 4\pi r^2 h(r) \frac{\sin Kr}{Kr} dr . \tag{8}$$

Here $P(K)$ and $S(K)$ are the so-called particle scattering factor and the structure factor, respectively.

C. Polydisperse particle and structure factors

For small concentrations one may write for the intensity, instead of Eq. (5),

$$R_0(K) = \rho \overline{f^2}\, \overline{P}(K) , \tag{9}$$

where

$$\rho = \sum_{i=1}^{p} \rho_i , \tag{10}$$

$$\overline{f^2} = \frac{\sum_{i=1}^{p} \rho_i f_i^2}{\sum_{i=1}^{p} \rho_i} , \tag{11}$$

$$\overline{P}(K) = \frac{\sum_{i=1}^{p} \rho_i f_i^2 B_i^2(K)}{\sum_{i=1}^{p} \rho_i f_i^2} , \tag{12}$$

at $K \to 0$, $\overline{P}(K) \to 1$.

For finite concentrations we now define an average structure factor by analogy with Eq. (6), i.e.,

$$R(K) = \rho \overline{f^2}\, \overline{P}(K) \overline{S}(K) \tag{13}$$

or combining Eq. (13) with Eq. (3):

$$\overline{S}(K) = \frac{\sum_{i,k=1}^{p} f_i f_k B_i(K) B_k(K) (\rho_i \rho_k)^{1/2} [\delta_{ik} + \tilde{H}_{ik}(K)]}{\sum_{i=1}^{p} \rho_i f_i^2 B_i^2(K)} . \tag{14}$$

Other definitions are possible, but the advantage of the definition of $\overline{S}(K)$ in Eq. (14) is that it can be compared directly with experiments performed at high and low concentrations, i.e.,

$$\overline{S}(K) = \frac{R(K)}{R_0(K)} \left(\frac{\rho_0}{\rho}\right) , \tag{15}$$

where ρ/ρ_0 is the dilution factor.

Note that Eq. (14) describes the scattering behavior of a p-component fluid mixture. For a truly polydisperse fluid the number of components p becomes very large and all summations, such as in Eq. (14), may be replaced by integrations. However, in the present paper we shall always be dealing with finite systems of N particles. The number of components p is then at most equal to N.

It should be kept in mind that $\overline{S}(K)$ is no longer a quantity that can be defined independently of the $B_i(K)$ as in a single-component fluid: Eq. (8). This will become apparent from the results in a subsequent section. On the other hand $\overline{S}(K)$ may contain information on the particle scattering factor which is useful, for instance because the dilute limit is beyond the reach of experiment, as in some aggregation colloids.

III. HARD-SPHERE PAIR POTENTIAL

The hard-sphere pair potential is defined by

$$U_{ik}(r) = \begin{cases} +\infty & \text{for } 0 < r < \dfrac{d_i + d_k}{2} \\ 0 & \text{for } r \geq \dfrac{d_i + d_k}{2} \end{cases} . \tag{16}$$

Here d_i and d_k are the hard-sphere diameters associated with the particle species i and k ($i, k = 1,...p$). No exact, analytical results for the $h_{ik}(r)$ are known for this potential at finite concentrations. Approximate theories, however, have been developed and fairly accurate results for hard spheres are predicted by the Percus–Yevick theory.

Explicit solutions of $h_{ik}(r)$ cannot be obtained, but it is possible to express the scattering properties in terms of auxiliary functions $q_{ik}(r)$ related to the so-called direct correlation function $c_{ik}(r)$ and which have a relatively simple algebraic form.[8]

In this way explicit, analytical solutions for the intensity $R(K)$ can be formulated for any number, p, of hard-sphere components. In an earlier publication[11] results were presented of the calculation of scattering intensities for a Schulz distribution of hard-sphere diameters. As a check on the computer program,[17] we verified numerically that for $p = 1$

the single-component results were reproduced and that for $p = 2$ the results were identical to those of Ashcroft and Langreth[14] for the two-component case.[15] For details we refer to previous papers.[9,11] For the convenience of the reader we have given the final equation in the Appendix.

IV. COMPUTER SIMULATIONS

The Monte Carlo simulations were carried out on a system of 108 polydisperse hard spheres. At the beginning of a series of MC runs the particle diameters d_i were chosen at random from a log-normal distribution.

$$P(\ln d)\mathrm{d}\ln d = (2\pi\beta^2)^{-1/2} \times \exp(-[\ln(d/d_0)]^2/2\beta^2)\mathrm{d}\ln d, \tag{17}$$

where β is a parameter controlling the width of the distribution. The unit of volume in our simulation was chosen as $\bar{d}^3 = \Sigma_i \rho_i d_i^3/\Sigma_i \rho_i$. The advantage of this choice is that it leads to the same relation between packing fraction $\phi = \pi/6\,\Sigma_i \rho_i d_i^3$ and number density $\rho = \Sigma_i \rho_i$ as in the monodisperse case, viz. $\phi = (\pi/6)\rho$. Initially the spheres that were put on the fcc lattice expanded sufficiently so that no two spheres overlapped. Thereon the system was "melted" and compressed (or expanded) to the desired density. Next the polydisperse fluid was left to equilibrate for $\sim 10^3$ Monte Carlo sweeps (= moves/particle). Particle displacements were generated by moving a particle randomly in a cube of edge length Δ around its original position. The move was accepted if no hard-core overlaps resulted from this displacement. The value of Δ was chosen such that $\sim 25\%$ of all trial moves are accepted. Note that we took Δ the same for all particles. It seems likely that sampling could be made more efficient by choosing a value of Δ that depends on the diameter of the particle to be moved. A typical Monte Carlo run consisted of 2.10^4 sweeps, excluding equilibration. In order to compute the structure factor for different form factors, we used a fast Fourier routine, i.e., we first computed the scattering amplitude $A(K)$ as:

$$A(K) = \sum_{i=1}^{N} f_i B_i(K)\exp(i\mathbf{K}\cdot\mathbf{r}_i). \tag{18}$$

$A(K)$ is related to $R(K)$ [Eq. (3)] by:

$$R(K) = V^{-1}\langle |A(K)|^2\rangle. \tag{19}$$

There is a twofold reason why we opted for the fast Fourier transform method to compute $R(K)$, rather than for the more usual procedure of accumulating a correlation function {$\rho[g(r) - 1]$ for monodisperse systems} during the run and performing the Fourier transform afterwards. First of all, for particles that are not point scatterers, accumulating the relevant scattering amplitude density correlation function is extremely time consuming. Secondly, in order to avoid truncation errors in the Fourier transform of such correlation functions one must introduce an assumption about the behavior or $g(r)$ (or the corresponding correlation function) for $r > L/2$, where L is the diameter of the periodic unit box in the simulation. But, as we are interested in the behavior of $R(K)$ at small K, we would rather not introduce such an assumption. We therefore compute $A(K)$ by direct Fourier transform of the scattering amplitude density. In the transform we take a spatial resolution of 256 points in the direction of $\mathbf{K}$. This number of points is sufficient to suppress aliasing effects, even for point scatterers. In order to improve our statistics we compute $A(K)$ for $\mathbf{K}$ along 13 independent directions [three along $P([100])$, six along $P([110])$, and four along $P([111])$, where P stands for all independent permutations]. We never found evidence for systematic differences between $R(K)$ along different directions, which is surprising in view of the small system size used. Simulations and calculations of the scattering amplitude $A(K)$ were performed for several particle scattering functions. Here we report results for: (a) homogeneous spheres where $f_i = d_i^3$ and $\zeta_i(r) = 1$ for $0 < r < \frac{1}{2}d_i$ and $\zeta_i(r) = 0$ for $r > \frac{1}{2}d_i$ substituted in Eq. (1) for $B_i(K)$; (b) infinitely thin shells where $f_i = d_i^2$ and $\zeta_i(r)$ is a delta peaked function for $r = \frac{1}{2}d_i$, so Eq. (1) gives: $B_i(K) = \sin(\frac{1}{2}Kd_i)/(\frac{1}{2}Kd_i)$. The 13×4 fast Fourier transforms were carried out every ten sweeps. This resulted in a moderate ($\sim 30\%$) increase in computing time. In order to get an estimate of the accuracy of the results we computed block averages of $R(K)$. The estimated error varies between 2% and 5%. In order to test whether a single sample drawn from the log-normal distribution of particle sizes is indeed representative of that particular distribution we carried out simulations with other samples drawn from the same distribution.

In the following section we present some results obtained for the scattering of homogeneous spheres and shells, as these are of the most physical interest.

V. RESULTS AND DISCUSSION

A. Monodisperse system

As a first test of the method we computed the structure factor for monodisperse hard spheres. We find that the results for $S(K)$ agree rather well with the approximate Percus–Yevick expression (see Figs. 2 and 5), except for the well-known fact that the PY expression tends to overestimate the height of the first peak in $S(K)$ and to underestimate the compressibility, i.e., $S(0)$. Less is known about the deviations of $S(K)$ from the PY theory in the small-K regime. We have attempted to fit the density dependence of $\ln[S(K)^{\mathrm{MC}}/S(K)^{\mathrm{PY}}]$ to a power series in K^2 for $K \leqslant \pi/\sigma$. As the PY theory is exact up to terms of order ρ^3, we have fitted the coefficients of powers of K^2 to a polynomial in the density with powers larger than three. However, apart from the well-known fact that the PY compressibility [i.e., $S(K = 0)$] is too low at high densities, our data were insufficiently accurate to reveal other systematic deviations from the PY expression in the small-K regime.

B. Comparison of simulations with the Percus–Yevick theory for polydisperse system

Four (discrete) diameter distributions were used, sampled at random from a log-normal distribution with $\beta = 0.1$; 0.2; 0.3, and 0.8. {The corresponding standard deviations $s_d = [(\bar{d^2} - \bar{d}^2)/\bar{d}^2]^{1/2} = [\exp(\beta^2) - 1]^{1/2}$ are s_d

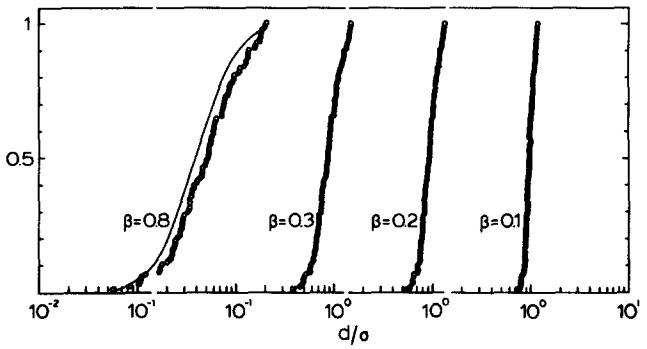

FIG. 1. Cumulative, discrete distributions of 108 hard-sphere diameters sampled from log-normal distributions. The parameter β is a measure of the width of the distribution (and is nearly equal to the standard deviation, see the text). The drawn curves correspond to the continuous cumulative distribution obtained by integrating Eq. (17). For all cases except $\beta = 0.8$, the continuous curve and the discrete sample coincide. For $\beta = 0.8$ the discrete distribution is shifted in such a way that the condition $\overline{d^3} = 1$ is satisfied.

$= 0.100; 0.202; 0.307; 0.947.\}$ The (cumulative) diameter distributions of the 108 spheres are shown in Fig. 1. For $\beta = 0.8$ we also carried out the MC simulations for a second sample of particle diameters drawn from the same distribution (not shown in Fig. 1). Distances are expressed in the following length unit:

$$\sigma = \overline{d^3}^{1/3} = \left[\frac{\sum_i \rho_i d_i^3}{\sum_i \rho_i}\right]^{1/3}; \tag{20}$$

simply denoted by the symbol σ. The PY calculations were performed with the same discrete distributions as used in the MC simulations.

Structure factors for a volume fraction $\phi = 0.3$ are shown in Figs. 2 and 4. Here ϕ is defined by the following equation:

$$\phi = \left(\frac{\pi}{6}\right) \sum_{i=1}^{P} \rho_i d_i^3 . \tag{21}$$

In Figs. 2 and 5 the scattering entities are homogeneous spheres with a scattering diameter equal to the hard-sphere diameter. In Fig. 4 the scattering entities are infinitely thin shells with the same diameters.

Figure 2 shows the following features:

(i) There is a main maximum at $K\sigma \approx 6$ which becomes less pronounced with increasing β, and appears to shift slightly to lower wave vectors.

(ii) In addition, the subsidiary oscillations in $\overline{S}(K)$ for $K\sigma > 6$ are progressively washed out. This loss of structure with increasing β is not surprising because the oscillations in $S(K)$ for a monodisperse system are mainly due to the sharp peak in $g(r)$ at $r = \sigma$. This peak is washed out in a mixture of particles with different diameters.

(iii) For polydisperse systems the value of $S(K = 0)$ is no longer equal to the osmotic compressibility as in the monodisperse case. Nevertheless, $S(K = 0)$ can still be used as an approximate measure of the compressibility of the polydisperse fluid. The fact that $\overline{S}(K = 0)$ remains small as β increases reflects the fact that the system remains difficult to compress. The relation between $S(K = 0)$ and the osmotic compressibility has been discussed in some detail in Ref. 16.

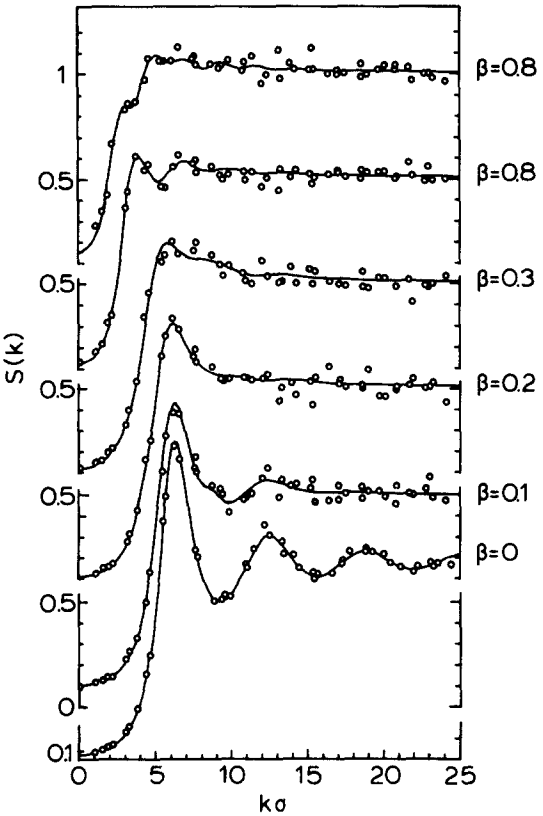

FIG. 2. Average structure factors for 108 homogeneous scattering spheres with diameters equal to those of the hard spheres. The scaling distance σ is defined as $(\overline{d^3})^{1/3}$. The upper curve is a *second* sample taken from a log-normal distribution of $\beta = 0.8$. The volume fraction $\phi = 0.3$.

(iv) The simulations fit closely to the PY calculation for small K and become noisier for large K, although the relative noise remains approximately constant.

(v) The two uppermost curves show $S(K)$ for different samples with the same β. This indicates that for broad distributions a sample of 108 particles becomes too small to represent the (smooth) log-normal distribution. Simulations with each of the discrete samples, however, again compare well with the PY calculations corresponding to that sample.

We took a special look at the behavior of $S(K)$ at small K (see Fig. 3). This range of K is interesting because it is often accessible to light-scattering experiments on colloids. In dilute systems the range of K is known as the "Guinier" range and a plot of $\log[R(K)]$ vs K^2 is usually referred to as a Guinier plot. The (negative) slope is a measure of the radius of gyration of the scattering particle, $[P(K) = \exp(-K^2 r_g^2/3)]$. At finite concentration (here $\phi = 0.3$), $S(K)$ increases linearly for small K^2 and shows a positive slope. Thus the change in slope of $\log[R(K)]$ as a

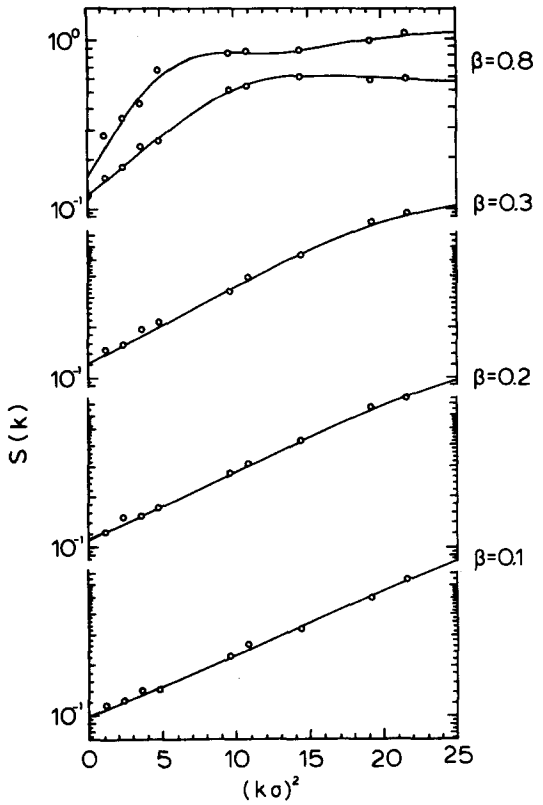

FIG. 3. The small-K part of the $\overline{S}(K)$ in Fig. 2 plotted as $\log[\overline{S}(K)]$ vs $K^2\sigma^2$.

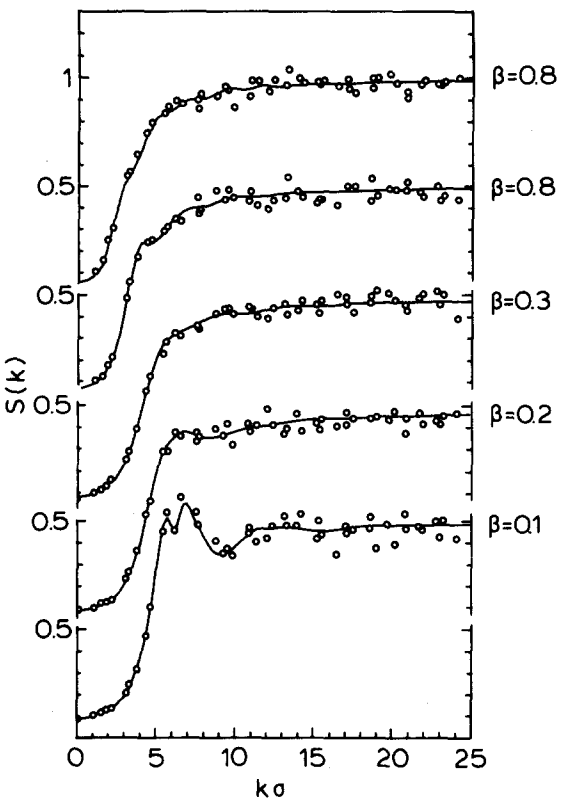

FIG. 4. Meaning of symbols as Fig. 2, but for thin scattering shells (constant thickness) with diameters equal to those of the hard spheres.

function ϕ is a first measure of the range of the interactions [the fourth moment of $h(r)$].

The results of Fig. 3 show that in the Guinier range the PY theory is followed closely, within the accuracy of the simulations, which is between 2%–5%. [It is known that for $\phi = 0.3$ and a monodisperse system, the PY theory gives a value for $(K = 0)$ which is 4% too low.[12]]

Let us now turn to Fig. 4 which gives the scattering of the thin shells. In the first place one notes the large influence of the different B_i on the shape of $\overline{S}(K)$ even for $\beta = 0.1$. [Note that for $\beta = 0$, $S(K)$ is unique and does not differ for spheres and shells.] The most salient feature in Fig. 4 is the disappearance of the main peak of $S(K)$. The reason for this behavior is that the form factor of a shell interferes more severely with the structure factor of the fluid than the form factor of a homogeneous sphere. For $\beta > 0.2$ the function goes monotonically to one.

Finally we consider some results for $\phi = 0.50$, a volume fraction where it is known that for monodisperse systems perceptible deviations from PY theory occur; e.g., for $S(K = 0)$ and $\beta = 0$ the PY approximation predicts a value which is about 12% too low.

Results are given in Fig. 5. One observes that for $\beta = 0.1$ again the simulation closely follows the PY result, except possibly at the top of the main peak. For $\beta = 0.20$ and $\beta = 0.30$ there are discrepancies between the main peak and the secondary extremum. In this figure we added results for a second run on the same assembly of spheres. Differences between the two sets of points are due to the statistical noise in the individual simulated points.

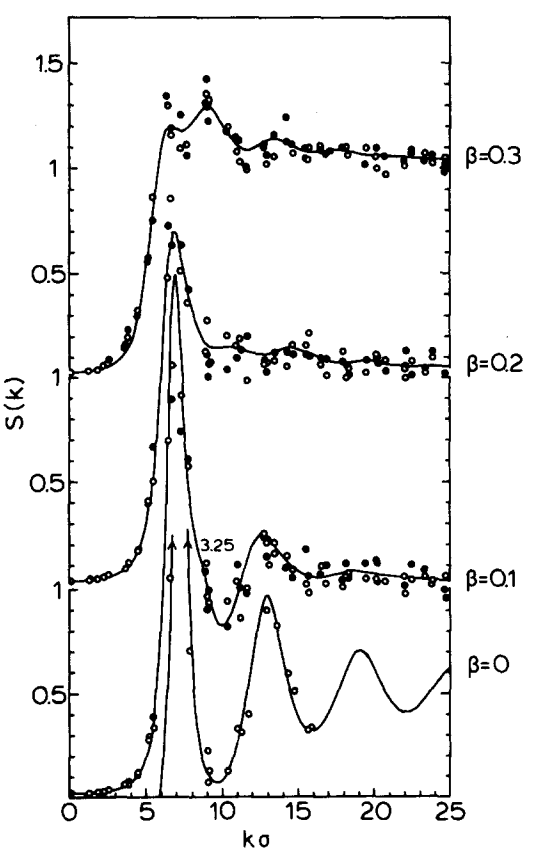

FIG. 5. Meaning of symbols as Fig. 2, but for $\phi = 0.5$. Results are for two different runs on the same assembly of spheres. The spread in the results is a measure for the inaccuracy in the simulation data.

This observation also applies to the small-K results where the fluctuations in the simulations are larger than in Fig. 3 with $\phi = 0.3$ It is still possible, however, that larger oscillations near the position of the main peak would be more real than the weak oscillations predicted by PY. This will need further study.

One obvious question is whether a simpler description than the polydisperse PY equation can be used to account for the Monte Carlo data. For instance, a number of experimentalists analyze their scattering data using the assumption that positional polydispersity and polydispersity in the form factors are, to a first approximation, uncorrelated.[4,5] This leads to an expression for $\overline{S}(K)$ of the form:

$$\overline{S}(K) = 1 + \beta(K)[S_p(K) - 1] , \tag{22}$$

where

$$\beta(K) = \left(\sum_{i=1}^{p} \rho_i\right)\left[\sum_{i=1}^{p} \rho_i f_i^2 B_i^2(K)\right] \Big/ \left[\sum_{i=1}^{p} \rho_i f_i B_i(K)\right]^2 \tag{23}$$

and the "positional" structure factor $S_p(K)$ is given by:

$$S_p(K) = N^{-1} \sum_{i=1}^{N} \sum_{j=1}^{N} \exp[i\mathbf{K} \cdot (\mathbf{R}_i - \mathbf{R}_j)] . \tag{24}$$

We have carried out a few tests of Eq. (22) and found it to yield a rather poor description of the MC data, even at low polydispersity ($\beta \approx 0.1$). The discrepancy is worst at low K values. Because of the disappointing results obtained with Eq. (22) at low polydispersities we have not attempted to carry out the comparison for higher values of β.

APPENDIX

$$(\pi/6)R(K) = \langle f^2 B^2 \rangle + \langle d^3 f B \Phi \rangle (L_2 + L_2^*) + 3\langle d^2 f B \Psi \rangle (L_3 + L_3^*) + \langle A A^* \rangle . \tag{A1}$$

Here, L_2, L_3, and A are complex quantities. Their complex conjugates L_2^*, L_3^*, and A^* are obtained by replacing i, the imaginary unit, by $-i$. Further,

$$L_2 = T_2/T_1;\ L_3 = T_3/T_1 , \tag{A2}$$

$$T_1 = F_{11}F_{22} - F_{12}F_{21} , \tag{A3}$$

$$T_2 = F_{21}\langle dfBe^{iX} \rangle - F_{22}\langle fBe^{iX} \rangle , \tag{A4}$$

$$T_3 = F_{12}\langle fBe^{iX} \rangle - F_{11}\langle dfBe^{iX} \rangle , \tag{A5}$$

$$F_{11} = 1 - \xi_3 + \langle d^3 \Phi e^{iX} \rangle , \tag{A6}$$

$$F_{12} = \langle d^4 \Phi e^{iX} \rangle , \tag{A7}$$

$$F_{22} = 1 - \xi_3 + 3\langle d^3 \Psi e^{iX} \rangle , \tag{A8}$$

$$F_{21} = \tfrac{1}{2}(1 - \xi_3)iK - 3\xi_2 + 3\langle d^2 \Psi e^{iX} \rangle , \tag{A9}$$

$$\Psi_k = (\sin X_k)/X_k , \tag{A10}$$

$$\Phi_k = (3/X_k^3)(\sin X_k - X_k \cos X_k) , \tag{A11}$$

$$A_k = d_k^3 \Phi_k L_2 + 3d_k^2 \Psi_k L_3 , \tag{A12}$$

$$X_k = \tfrac{1}{2} K d_k . \tag{A13}$$

The brackets indicate averages over diameters, i.e.,

$$\langle y \rangle \equiv (\pi/6) \sum_{k=1}^{p} \rho_k y(d_k) , \tag{A14}$$

where $y(d)$ is any function of d. Examples are

$$\langle f^2 B^2 \rangle = (\pi/6) \sum_{k=1}^{p} \rho_k f_k^2 B_k^2 , \tag{A15}$$

$$\langle fBd^2 \Psi \rangle = (\pi/6) \sum_{k=1}^{p} \rho_k f_k B_k d_k^2 \Psi_k , \tag{A16}$$

$$\langle dfBe^{iX} \rangle = (\pi/6) \sum_{k=1}^{p} \rho_k d_k f_k B_k e^{iX_k} , \tag{A17}$$

$$\langle dfBe^{iX} \rangle^* = (\pi/6) \sum_{k=1}^{p} \rho_k d_k f_k B_k e^{-iX_k} . \tag{A18}$$

In particular,

$$\xi_\nu = (\pi/6) \sum_{k=1}^{p} d_k^\nu \rho_k = \langle d^\nu \rangle . \tag{A19}$$

Thus ξ_3 is the overall volume fraction of spheres. Further,

$$B_k(K) = f_k^{-1} \int_0^\infty 4\pi r^2 \zeta_k(r) \frac{\sin Kr}{Kr} dr , \tag{A20}$$

$$f_k = \int_0^\infty 4\pi r^2 \zeta_k(r) dr , \tag{A21}$$

where $\zeta_k(r)$ is the (spherically symmetric) distribution of scattering amplitude in particle k as a function of the distance from the center of the hard sphere k.

[1] See, for example, J. B. Hayter, Faraday Discuss. Chem. Soc. **76**, 7 (1983); A. Vrÿ *et al.*, *ibid.* **76**, 19 (1983); D. J. Cebula *et al.*, *ibid.* **76**, 37 (1983); J. D. F. Ramsay *et al.*, *ibid.* **76**, 53 (1983).
[2] A. K. van Helden, J. W. Jansen, and A. Vrij, J. Colloid Interface Sci. **81**, 354 (1981).
[3] D. J. Cebula, R. H. Ottewill, J. Ralston, and P. N. Pusey, J. Chem. Soc. Faraday Trans. 1 **77**, 2585 (1981).
[4] J. B. Hayter, Faraday Discuss. Chem. Soc. **76**, 7 (1983).
[5] M. Kotlarchyk and S. H. Chen, J. Chem. Phys. **79**, 2461 (1983).
[6] A. K. van Helden and A. Vrij, J. Colloid Interface Sci. **78**, 312 (1980).
[7] J. L. Lebowitz, Phys. Rev. A **133**, 895 (1964).
[8] R. J. Baxter, J. Chem. Phys. **52**, 4559 (1970).
[9] (a) A. Vrij, J. Chem. Phys. **69**, 1742 (1978); (b) **71**, 3267 (1979).
[10] L. Blum and G. Stell, J. Chem. Phys. **71**, 42 (1979); **72**, 2212 (1980).
[11] P. van Beurten and A. Vrij, J. Chem. Phys. **74**, 2744 (1981).
[12] J. P. Hansen and I. R. McDonald, *Theory of Simple Liquids* (Academic, London, 1976).
[13] G. Fournet, as cited in A. Guinier and G. Fournet, *Small Angle Scattering of X rays* (Wiley, New York; Chapman and Hall, London, 1955), p. 65.
[14] N. W. Ashcroft and D. C. Langreth, Phys. Rev. **156**, 685 (1967).
[15] We thank Dr. J. B. van Tricht for doing some calculations for us.
[16] A. Vrij, J. Colloid Interface Sci. **90**, 110 (1982).
[17] A listing of the computer program can be obtained from one of the authors (A. V.).